THE JOURNAL OF BIOLOGICAL CHEMISTRY VOL. 290, NO. 11, pp. 6755–6762, March 13, 2015

Identification of FAH Domain-containing Protein 1 (FAHD1) as Oxaloacetate Decarboxylase*

Received for publication, September 4, 2014, and in revised form, January 7, 2015 Published, JBC Papers in Press, January 9, 2015, DOI 10.1074/jbc.M114.609305

Haymo Pircher[‡], Susanne von Grafenstein[§], Thomas Diener[‡], Christina Metzger[‡], Eva Albertini[‡], Andrea Taferner[‡], Hermann Unterluggauer[‡], Christian Kramer[§], Klaus R. Liedl[§], and Pidder Jansen-Dürr[‡1]

From the [‡]Institute for Biomedical Aging Research and Center for Molecular Biosciences Innsbruck (CMBI), Universität Innsbruck, Rennweg 10, 6020 Innsbruck and the [§]Institute for General, Inorganic and Theoretical Chemistry and Center for Molecular Biosciences Innsbruck, Universität Innsbruck, Innrain 80-82, 6020 Innsbruck, Austria

Background: Enzymes of the FAH superfamily catalyze a multitude of diverse chemical reactions.
Results: Using molecular modeling followed by biochemical investigations, FAHD1 was identified as oxaloacetate decarboxylase.
Conclusion: Our findings suggest that ODx activity can be found in eukaryotic members of the FAH superfamily.
Significance: Our results identify a mammalian ODx enzyme as a so far undescribed player in mitochondrial metabolism.

Fumarylacetoacetate hydrolase (FAH) domain-containing proteins occur in both prokaryotes and eukaryotes, where they carry out diverse enzymatic reactions, probably related to structural differences in their respective FAH domains; however, the precise relationship between structure of the FAH domain and the associated enzyme function remains elusive. In mammals, three FAH domain-containing proteins, FAHD1, FAHD2A, and FAHD2B, are known; however, their enzymatic function, if any, remains to be demonstrated. In bacteria, oxaloacetate is subject to enzymatic decarboxylation; however, oxaloacetate decarboxylases (ODx) were so far not identified in eukaryotes. Based on molecular modeling and subsequent biochemical investigations, we identified FAHD1 as a eukaryotic ODx enzyme. The results presented here indicate that dedicated oxaloacetate decarboxylases exist in eukaryotes.

The fumarylacetoacetate hydrolase (FAH)[2] protein superfamily branches out through all organisms, from prokaryotes to humans, comprising a diverse set of enzymatic functions. Its distinguishing feature is the highly conserved catalytic center designated as the FAH fold. It is named after the founding member of the family, the well characterized mammalian enzyme FAH, which hydrolyzes fumarylacetoacetate to fumarate and acetoacetate (1), constituting the last step in the metabolic breakdown of tyrosine. In the genetic disorder hereditary tyrosinemia type 1, this reaction is compromised due to mutations in the FAH gene (2). The accumulation of toxic metabolites caused by the disruption of FAH activity leads to severe liver and renal disease (3).

Although the FAH fold is highly conserved, FAH superfamily members cover a wide range of diverse enzymatic activities. Several members possess β-diketone hydrolase activity, including FAH itself. HpcE from *Escherichia coli* is a bifunctional decarboxylase/isomerase, catalyzing the decarboxylation of 2-oxo-5-carboxy-hept-3-ene-1,7-dioic acid to 2-hydroxy-hepta-2,4-diene-1,7-dioic acid, followed by the conversion into 2-oxo-hept-3-ene-1,7-dioic acid (4). Other members that were characterized in both structure and enzymatic function include KdaD from *Sulfolobus solfataricus* (5), dehydrating 2-keto-3-deoxy-D-arabinonate to 2,5-dioxopentanoate, and MhpD from *E. coli* (6), which hydrates 2-hydroxypenta-2,4-dienoic acid to 4-hydroxy-2-ketopentanoic acid. Overall, the FAH superfamily includes many prokaryotic members with very distinct functions that lack homologs in eukaryotes. This can be explained by the fact that these enzymes are part of highly specialized metabolic pathways, involving chemical compounds that higher organisms are unable to convert and utilize for their metabolism (5). One recently identified prokaryotic member of the FAH superfamily found in *Corynebacterium glutamicum*, referred to as Cg1458, was characterized as a novel soluble oxaloacetate decarboxylase (ODx) (7, 8); however, eukaryotic ODx enzymes were not identified so far.

Besides FAH itself, two other members of the superfamily have been described in humans, FAHD1 and FAHD2, with orthologs in most eukaryotic organisms. The 25-kDa FAH domain-containing protein 1 (FAHD1) has been studied by x-ray crystallography (9), revealing a homodimeric structure and a mixed β-sandwich roll fold bearing a metal ion binding site, similar to other members of the FAH protein family. At that time, there were no further publications about FAHD1, and its enzymatic function was still unknown. Based on the structure of the active site, a hydroxylase or decarboxylase function was proposed. Also, a common function shared with other so far uncharacterized FAH proteins, *E. coli* YcgM and *Thermus thermophilus* TTHA0809, was suggested due to structural similarities (9). FAHD2 shows moderate sequence homology with FAHD1, but no further data are available for this enzyme at the moment.

* This work was supported by a grant from the Austrian Science Funds (FWF; NFN S93) (to P. J.-D.) and by the European Union through the FP6 Integrated Project MiMAGE (to P. J.-D.).
[1] To whom correspondence should be addressed. Tel.: 43-512-507-50844; E-mail: pidder.jansen-duerr@uibk.ac.at.
[2] The abbreviations used are: FAH, fumarylacetoacetate hydrolase; FAHD1, fumarylacetoacetate hydrolase domain-containing protein 1; ODx, oxaloacetate decarboxylase; PC, pyruvate carboxylase; PEPCK, phosphoenolpyruvate carboxykinase.

Due to the broad range of enzymatic functions present within the FAH superfamily despite the structural similarities, it proved challenging to narrow down possible functions for FAHD1 from sequence and structural information. In a recent study (10), we utilized a bioinformatics approach to show for the first time that FAHD1 is closely related to the prokaryotic fumarylpyruvate hydrolase NagK (11). This finding was derived from the fact that charged residues present in the catalytic center of FAHD1 and likely involved in its enzymatic function (9) are fully conserved between NagK and FAHD1. Enzymatic assays performed with the purified protein confirmed that FAHD1 is able to hydrolyze substrates of the acylpyruvate class *in vitro*. In the case of acetylpyruvate, V_{max} was determined as 0.14 μmol min^{-1} mg^{-1}, with a K_m value of 4.6 μM. The reaction rate was found to be dependent on the type of the bound divalent metal ion, with Mg^{2+} and Mn^{2+} yielding the highest rates. Immunoblot analysis indicated widespread expression of FAHD1 in various murine tissues, with highest expression in kidney and liver, as well as in a wide range of human cell lines; immunofluorescence studies showed clear mitochondrial localization (10).

As there is no existing evidence that acylpyruvates play any significant role in the metabolism of higher organisms, the *in vivo* relevance of the acylpyruvase activity associated with FAHD1 still awaits confirmation. In this study, we conducted a further search for possible *in vivo* substrates by means of bioinformatics and structural modeling, trying to clarify the relevance of FAHD1 for mammalian metabolism.

EXPERIMENTAL PROCEDURES

Structural Investigation of the FAH Domain Active Sites—The Protein Data Bank (PDB) database (12) was screened for entries associated with the Pfam accession number PF01557 to identify the FAH family. The 32 resulting entries were structurally compared in the Molecular Operating Environment (MOE) software (Chemical Computing Group, MOE release 2013.08, Montreal, Canada). The study was limited to chain A of PDB entries containing multiple structures in a unit cell. Superposition of the proteins was first performed based on all C-α atoms. Subsequently, a refined superposition on residues within 9 Å around the Mg^{2+} ion in 1SAW was performed. This inner sphere was defined as the active site. Structural similarity is calculated based on the root mean square deviation of C-α atom positions included within this sphere. Low values of root mean square deviation indicate very similar structures. Based on the similarity matrix between the 32 structures, a hierarchical clustering was performed resulting in a tree representation of FAH relations.

Modeling of FAHD1 Active Site—The x-ray structure of human FAHD1 (PDB code 1SAW) (9, 13) lacks 11 highly flexible residues next to the active site (Asp-29 to Leu-39). We constructed this region using the "Loop modeler" tool of MOE. To allow the loop region to extend into the active site, as expected for a closed lid conformation, four water positions were deleted in the active site: HOH314, HOH316, HOH356, and HOH359. The missing loop was defined between Val-21 and Val-43 to identify potential loop candidates from the PDB. A tolerant maximal walk step of 5 amino acids allowed varying potential anchoring points between residue 16 and residue 48. All other parameters were kept as default. 94 structured loop regions were identified as potential templates with these parameters. We used the best scored candidate from the putative FAH protein from *Yersinia pestis* (PDB code 3S52) as the template structure for loop construction. The parameters for refined loop modeling included an adaption of the environment by side chain repacking (default parameters).

Bacterial Recombinant Expression and Purification of FAHD1—N-terminally His- and S-tagged versions of human wild-type FAHD1 and three mutants (H30A, E33A, and D102A/R106A) were recombinantly expressed in *E. coli* and purified as reported previously (10).

Oxaloacetate Decarboxylase Assay Utilizing Lactate Dehydrogenase and NADH—ODx activity was measured with an Infinite M200 spectrophotometer (Tecan) in a disposable UV cuvette (1-cm path length, Brand) at 25 °C. Each reaction was performed in 1 ml of assay buffer (50 mM Tris-HCl, 100 mM KCl, 1 mM $MgCl_2$, 200 μM NADH, pH 7.4) containing 12 μg of recombinant FAHD1 and 0.1 units of L-lactate dehydrogenase. The reaction was started by adding oxaloacetate to a final concentration of 100 μM. The decreasing absorbance of NADH was recorded between 300 and 380 nm in regular time intervals.

Direct Oxaloacetate Decarboxylase Assay—ODx activity was measured with an Infinite M200 spectrophotometer (Tecan), similar to Ran *et al.* (8). The assay was performed in a disposable UV cuvette (1-cm path length, Brand) at 25 °C in 1 ml of assay buffer (50 mM Tris-HCl, 100 mM KCl, 1 mM $MgCl_2$, pH 7.4) containing varying amounts of recombinant FAHD1 (3–60 μg). The reaction was started by adding oxaloacetate to a final concentration of up to 1 mM. The decreasing absorbance at 255 nm (ϵ = 1070 M^{-1} cm^{-1} for oxaloacetate) was measured over several minutes in regular time intervals and used to calculate initial reaction rates. For the inhibitor assay, varying concentrations of oxalate were included. All reactions were performed three times. Reaction mixtures containing no substrate were used as blank. All rates were corrected for appearance of pyruvate and for auto-decarboxylation under assay conditions (14).

Analysis of Oxaloacetate Decarboxylase Reaction by HPLC—1 ml of assay buffer containing oxaloacetate (1 mM) and purified recombinant FAHD1 protein (120 μg) was incubated at room temperature for 30 min. A control lacking FAHD1 was incubated analogously. The conversion mixture and control of the FAHD1 reaction were analyzed by HPLC using an ÄKTA purifier system (GE Healthcare) equipped with a Bio-Rad Aminex HPX-87H column (300 × 7.8 mm). Detection was at 210 nm. 84 μl of sample were injected and eluted with 5 mM H_2SO_4 as the eluent at a flow rate of 0.5 ml min^{-1} at room temperature. Identification of peaks was based on the characteristic retention times of high purity standards (>99%) of oxaloacetate and pyruvate.

Mouse Work—F2 generation C57BL/6 mice heterozygous for a LoxP-flanked FAHD1 gene were established by inGenious Targeting Laboratory. FAHD1$^{-/-}$ mice were generated by crossing FAHD1$^{flox/+}$ with Cre$^{0/+}$ transgenic mice followed by outcrossing of Cre alleles and crossing of FAHD1$^{-/+}$ mice. The knock-out was verified by PCR and immunoblot. The mice were housed in a temperature-controlled room at 22 °C with a

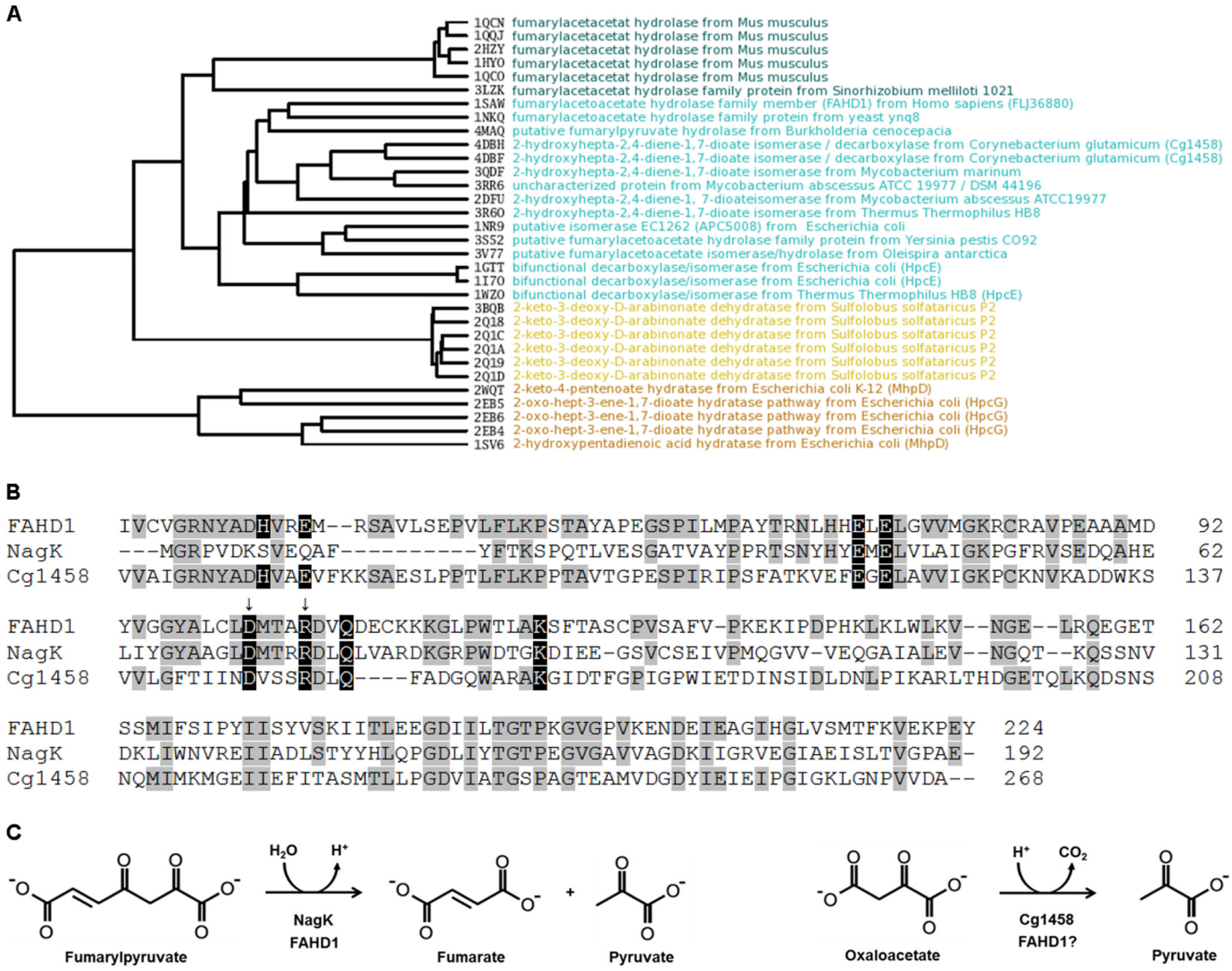

FIGURE 1. **Homology between FAHD1 and specific FAH family members.** *A*, root mean square deviation-based active site clustering between structures of different FAH domains indicates that FAHD1 from *Homo sapiens* (PDB code 1SAW) is more closely related to prokaryotic FAH domains (*cyan*) than to FAH from higher organisms (*dark cyan*, *e.g.* PDB code 2HCY). For the structural comparison of the multidomain enzyme HpcE, the C-terminal domain was considered in the alignment. The proteins MhpD and HpcG (*brown*) have the highest structural difference to FAHD1. The catalytic mechanism of these hydrating enzymes does not include the cleavage of a carbon-carbon bond. *B*, primary sequence alignment of human FAHD1 with functionally related members of the FAH superfamily. From *top* to *bottom*: *H. sapiens* FAHD1 (amino acids 20–224), *Ralstonia* sp. strain U2 NagK fumarylpyruvate hydrolase, *C. glutamicum* Cg1458 oxaloacetate decarboxylase (amino acids 63–268). Conserved amino acids shared with FAHD1 are marked in *gray*, and charged amino acids reported to be important for ODx activity in Cg1458 are marked in *black*. *Arrows* denote amino acids altered in the FAHD1 mutant. *C*, chemical structures and reaction schemes outlining the hydrolysis of fumarylpyruvate and the decarboxylation of oxaloacetate.

12-h light/12-h dark cycle. All mice were given unlimited access to water and standard chow (ssniff V1536-00). Individually housed male mice, aged 6–8 weeks, were divided into three groups; control mice were provided with standard chow *ad libitum*, and food was withdrawn for 18 h for fasted and refed mice, who were given access to standard chow for 4 h after fasting. Water was provided *ad libitum*. After the mice were sacrificed via cervical dislocation, desired organs were harvested, snap-frozen, and stored in liquid nitrogen.

Preparation of RNA and Quantitative Real Time PCR—Total RNA from mouse liver was isolated using TRIzol® reagent (Sigma) according to the manufacturer's protocol. For cDNA synthesis, 1 μg of total RNA was reverse transcribed with the RevertAid First Strand cDNA synthesis kit (Thermo Fisher Scientific) and diluted 1:5. Amplification was carried out with specific primers for *FAHD1*, *PC* (pyruvate carboxylase), and *PCK1* (phosphoenolpyruvate carboxykinase 1). Real time quantitative PCR was performed in triplicates using LightCycler® 480 SYBR Green I master mix (Roche Applied Science).

Western Blot—Frozen mouse organs were homogenized in PBS supplemented with protease inhibitors (one Complete Mini EDTA-free tablet per 10 ml, Roche Diagnostics). Lysate supernatants (30 μg of total protein) were separated by SDS-PAGE and blotted onto a PVDF membrane. Rabbit monoclonal anti-mouse FAHD1 antibody (purpose-made, 14 μg/ml), rabbit polyclonal anti-PEPCK antibody recommended for detection of PCK1 and PCK2 (Santa Cruz Biotechnology sc-32879, 1:2,000), rabbit polyclonal anti-PC antibody (Proteintech 16588-1-AP, 1:2,000), and anti-rabbit HRP-conjugated secondary antibody (Dako P0399, 1:2,500) were applied by standard

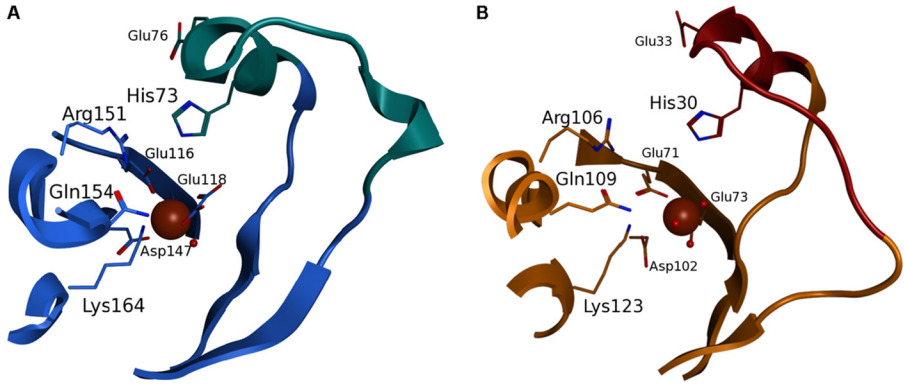

FIGURE 2. **Model generation of human FAHD1 with closed lid structure.** *A* and *B*, comparison of the conserved active site geometry of Cg1458 (*A*) and FAHD1 (*B*). The lid region (*cyan*) carrying the catalytic histidine and an activating glutamate residue is closed in Cg1458 upon binding of the inhibitor oxalate (shown as *sticks*). The model of the closed lid region in FAHD1 (*brown*) completes the active site of FAHD1 around the magnesium ion (*brown sphere*). Conserved residues around the active site are shown as *sticks* and labeled. Secondary structure elements are represented as graphic elements for Cg1458 and FAHD1 in *blue* and *orange*, respectively. Two water molecules (*red spheres*) are co-crystallized in FAHD1 at the binding site of the oxalate, suggesting a similar binding mechanism.

Western blot protocol. α-Tubulin antibody (Sigma T5168, 1:10,000) was used for loading control with an anti-mouse HRP-conjugated secondary antibody (Dako P0447, 1:20,000). Detection was achieved by ECL Prime (GE Healthcare). For relative protein quantification, specific bands were analyzed using Fiji software (15).

Analysis of Oxaloacetate Levels in Mouse Tissue—3-month-old female mice (wild-type and FAHD1$^{-/-}$ littermates) were sacrificed by cervical dislocation, and the desired organs (kidney and liver) were immediately excised and shock-frozen in liquid nitrogen. Frozen organs were homogenized in ice-cold 5% perchloric acid (1 ml per 100 mg of tissue) and assayed according to the method described by Parvin *et al.* (16). Briefly, after hydrolysis of endogenous acetyl-CoA and subsequent neutralization, a 25-μl aliquot was included in a 200-μl reaction containing 0.6 units of citrate synthase (Sigma) and 3 pmol of [^{3}H]acetyl-CoA (39 nCi, Moravek Biochemicals) to transform endogenous oxaloacetate into [^{3}H]citrate. After adsorption of unreacted [^{3}H]acetyl-CoA to activated charcoal (Sigma), samples were measured in a liquid scintillation counter (LS 6500, Beckman).

RESULTS

Identification of FAHD1 as Candidate Oxaloacetate Decarboxylase by Molecular Modeling—To systematically explore potential catalytic activities inherent to the FAH domain of FAHD1, we performed a detailed structural comparison of FAHD1 with 32 entries from the PDB assigned to the FAH superfamily (Fig. 1*A*). We focused the comparison on residues around the active site only as the structures of the FAH domains differ in various insertions extending from the FAH core. In this clustering by structural similarity, the human FAHD1 segregates in one branch together with FAH domains from lower organisms but not with FAH, the founding member of the FAH superfamily. One of the proteins within the same branch as FAHD1 was the oxaloacetate decarboxylase Cg1458 from *C. glutamicum* (Fig. 1*A*). The crystal structure of Cg1458 was described recently (8), and the importance of eight charged amino acids deemed vital for the enzymatic function was analyzed via mutants, resulting in mostly inactive variants. Sequence alignment of FAHD1 and Cg1458 reveals that all of these charged residues are conserved between the two enzymes, whereas only six of these amino acids are conserved in bacterial fumarylpyruvate hydrolase NagK (Fig. 1*B*). In Fig. 1*C*, the known catalytic activities of NagK, Cg1458, and FAHD1 are schematically depicted, as well as the hypothetical ODx activity of FAHD1. The catalytic mechanism of Cg1458 was derived from an x-ray structure with the inhibitor oxalate bound to the active site (8). Binding of the inhibitor induces the closure of a lid region over the binding site (Fig. 2*A*). This region contains the catalytic histidine residue stabilized by a glutamate residue essential for the activity. In the available structure of FAHD1, the corresponding region is missing, probably due to high mobility. By computational loop modeling utilizing a putative FAH family protein from *Y. pestis*, we propose a closed structure of FAHD1 where His-30 and Glu-33 complete the active site (Fig. 2*B*) in equivalence to the structure of Cg1458.

Oxaloacetate Decarboxylation by FAHD1 in Vitro—To confirm the hypothesis that FAHD1 exhibits ODx activity, we tested recombinant purified FAHD1 in a photometric assay by monitoring the follow-up reaction by lactate dehydrogenase metabolizing pyruvate (Fig. 3*A*). In this assay, FAHD1 showed ODx activity, which was clearly discernible from the observed rate of auto-decarboxylation (Fig. 3*B*). In a direct oxaloacetate decarboxylation assay, a V_{max} of 0.21 μmol min^{-1} mg^{-1} and a K_m value of 32 μM were determined for the wild-type enzyme (Fig. 3*C*). HPLC analysis, after incubation of the substrate in the presence or absence of the purified enzyme, confirmed the conversion of oxaloacetate to pyruvate by FAHD1 (Fig. 3*D*). A catalytically dead double mutant reported before (10) displayed only residual ODx activity, whereas mutation of loop residues His-30 and Glu-33, conserved and of known importance in Cg1458, led to a significant reduction in each case (Fig. 3*E*). To further characterize the ODx activity inherent to FAHD1, we used oxalate, an established inhibitor of Cg1485 (8). Indeed, oxalate caused potent competitive inhibition of oxaloacetate decarboxylation by FAHD1, with an inhibitor constant (K^I) of about 1 μM (Fig. 3*F*).

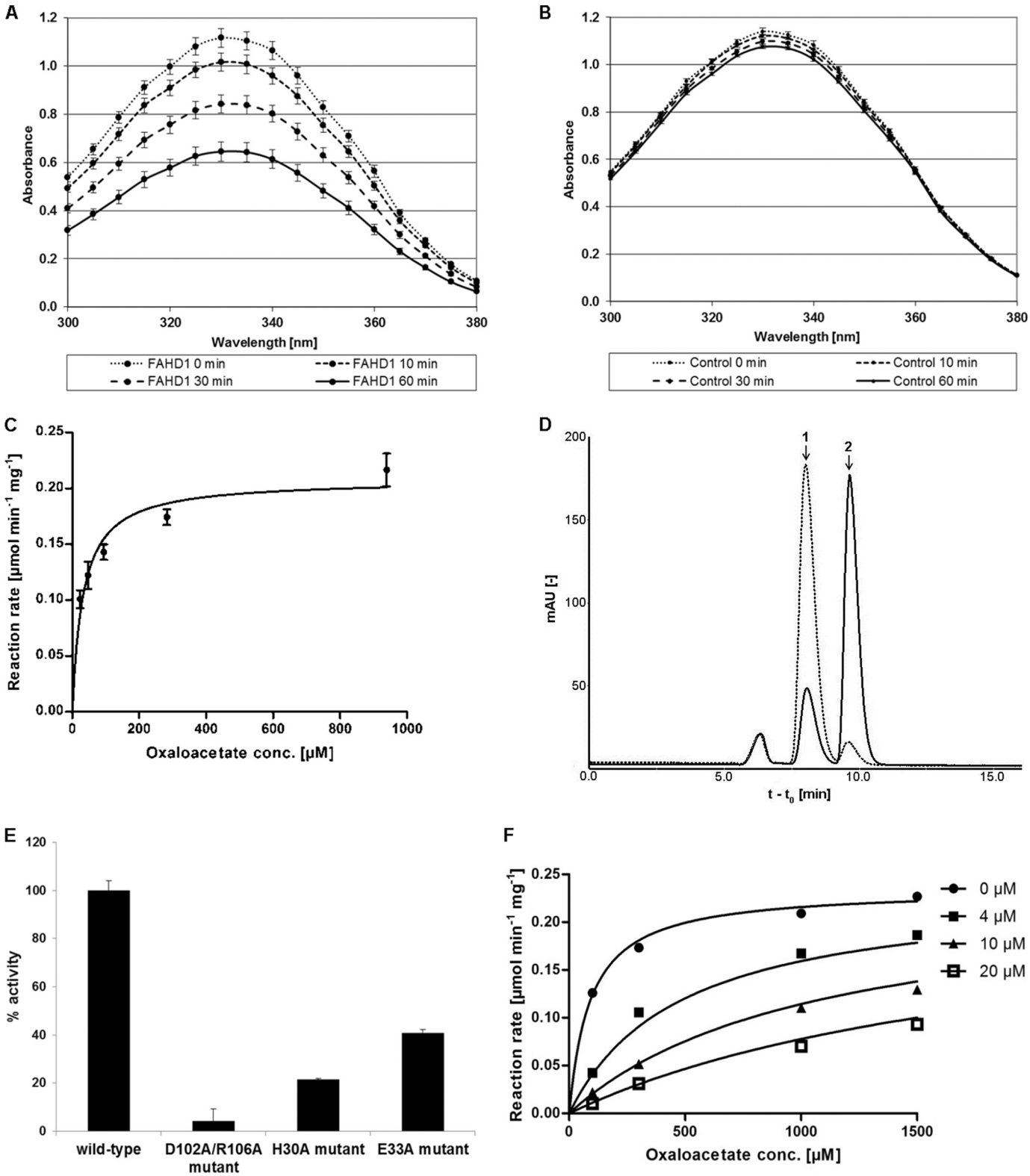

FIGURE 3. **Characterization of *in vitro* ODx activity of FAHD1.** *A* and *B*, degradation of 100 μM oxaloacetate at 25 °C in 1 ml of assay buffer by 12 μg of recombinant FAHD1 (*A*) or without enzyme (*B*). Actual curves show follow-up consumption of 200 μM NADH by lactate dehydrogenase metabolizing pyruvate. *C*, effect of substrate concentration on ODx reaction rate in the presence of purified FAHD1, determined by photometric analysis at 25 °C. Nonlinear regression analysis of Michaelis-Menten kinetics was performed with Prism 5 software (GraphPad Software). Data are represented as mean ± S.D. ($n = 3$). *D*, HPLC analysis of oxaloacetate breakdown in the presence (*solid line*) and absence (*dashed line*) of purified FAHD1. Retention times for oxaloacetate (*peak 1*) and pyruvate (*peak 2*) standards are indicated by *arrows*. *E*, ODx activity of wild-type FAHD1, and of several FAHD1 mutants. Data are represented as mean ± S.D. ($n = 3$). *F*, nonlinear regression analysis of inhibition by oxalate, performed with Prism 5 software ($K^I = 0.93$ μM, $R^2 = 0.99$). *Oxaloacetate conc.*, oxaloacetate concentration.

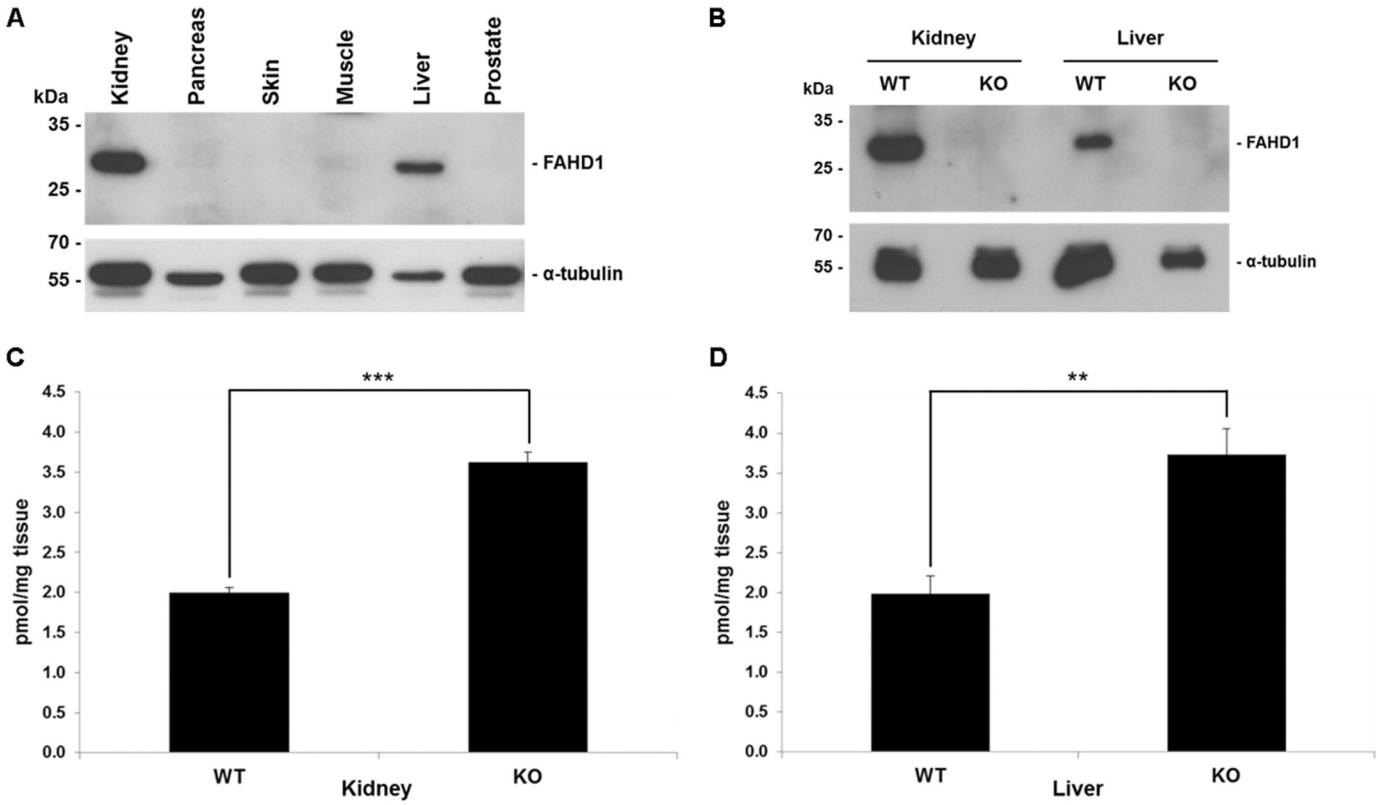

FIGURE 4. **Comparison of oxaloacetate levels in organs of WT and FAHD1 KO mice.** *A*, Western blot showing FAHD1 levels in wild-type mouse tissues. Tubulin levels are shown as loading control. *B*, Western blot confirming lack of FAHD1 protein expression in kidney and liver lysates of the FAHD1$^{-/-}$ mouse, with wild-type as control. *C* and *D*, oxaloacetate levels determined in kidney (*C*) and liver (*D*) extracts of 3-month-old female wild-type and FAHD1 knock-out mice. Data are represented as mean ± S.D. ($n = 3$). **, $p < 0.01$; ***, $p < 0.001$.

Expression and Evidence for in Vivo Activity in Mice—Previous studies, using a polyclonal antiserum raised against recombinant FAHD1 protein, indicated a widespread expression pattern for FAHD1 in many mouse tissues, based on two distinct bands revealed by Western blot (10). In view of the specific ODx activity for FAHD1 revealed here, the expression pattern of FAHD1 was reinvestigated by improved immunological reagents. In particular, we utilized a purpose-made monoclonal antibody to evaluate endogenous FAHD1 levels in a selection of mouse tissues by immunoblotting. FAHD1 was detected as a single band of apparent molecular mass of ~29 kDa, and among the tested tissues, expression was predominantly observed in kidney and liver (Fig. 4*A*). Decarboxylation of oxaloacetate was observed previously in extracts from rat liver mitochondria (17, 18); however, the identity of the protein(s) responsible for this activity has remained unclear and has not since been further investigated. To investigate whether oxaloacetate is a relevant *in vivo* substrate for FAHD1, the *FAHD1* gene was deleted in the mouse by homologous recombination, and FAHD1 knock-out was confirmed by Western blot of kidney and liver lysates (Fig. 4*B*). Metabolites were extracted from both the kidney and the liver of FAHD1$^{-/-}$ mice and wild-type littermates. The concentration of oxaloacetate in these extracts was determined in an enzymatic assay utilizing the reaction with ^{3}H-labeled acetyl-CoA to form citrate (16). The concentration of oxaloacetate was significantly increased in both the kidney (Fig. 4*C*) and the liver (Fig. 4*D*) of FAHD1$^{-/-}$ mice, indicating that oxaloacetate is indeed a relevant *in vivo* substrate for FAHD1 in mice. No other overt phenotypical alterations relative to wild type were observed in these mice, at least at young age.[3] This may be the consequence of compensatory mechanisms or a non-essential role of FAHD1 in mice, or it may depend on the nutritional and metabolic conditions the mice are experiencing.

Regulation of FAHD1 and Metabolically Related Genes—In light of the newly ascribed ODx function of FAHD1, expression levels may well be influenced by different metabolic states. To take a first look into possible regulatory effects, we compared the expression of *FAHD1*, *PC*, and phosphoenolpyruvate carboxykinase (*PEPCK*) during a fed/fasted/refed cycle in the mouse liver, on both the mRNA (Fig. 5*A*) and the protein level (Fig. 5, *B* and *C*). Unlike *PEPCK*, which is strongly up-regulated during fasting conditions on both the mRNA and the protein level, *FAHD1* showed only a very mild and marginally significant down-regulation of mRNA levels in fasted mice. *PC* mRNA was up-regulated during fasting, but this effect disappeared when looking at protein levels, as observed before (19).

DISCUSSION

The results reported here provide new insight into structure-function relationships within the superfamily of FAH domain-containing proteins. This family contains members with a large variety of distinct catalytic activities, many of which are how-

[3] H. Pircher, T. Diener, C. Metzger, E. Albertini, A. Taferner, and P. Jansen-Dürr, unpublished results.

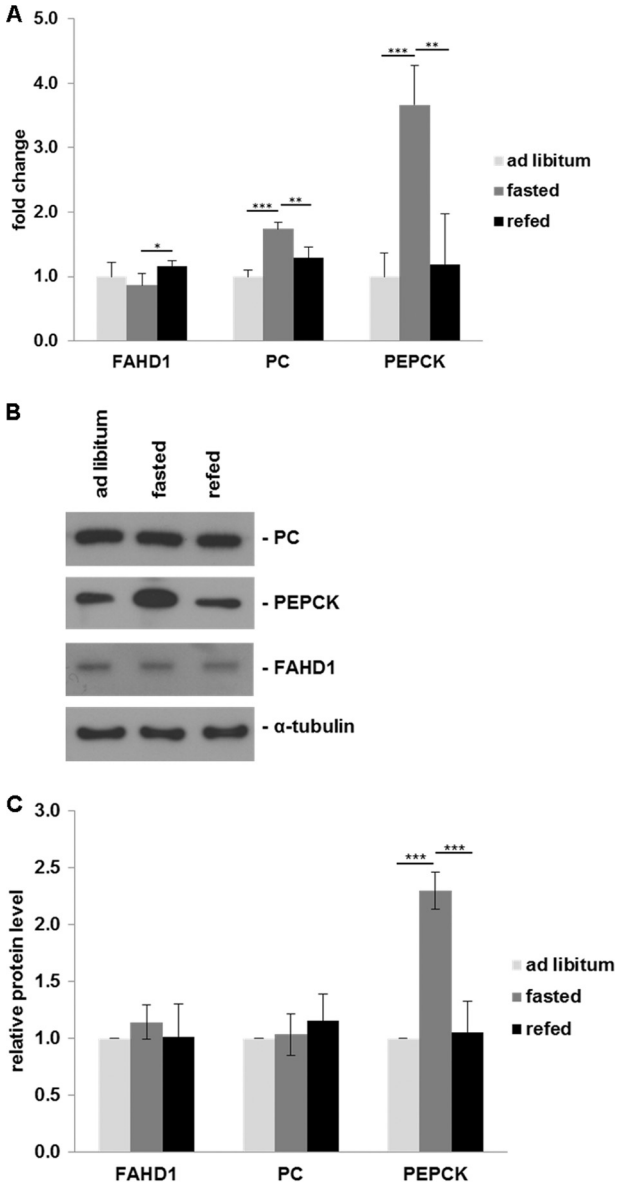

FIGURE 5. **Regulation of gene expression of selected enzymes during fed/fasted cycle.** *A*, mRNA expression of *FAHD1*, *PC*, and *PEPCK* was examined by real time quantitative PCR in the liver of *ad libitum* fed, fasted, and refed mice. For each gene, the fold induction of mRNA expression in fasted and refed mice as compared with *ad libitum* fed mice is indicated. Results indicate mean ± S.D. of three triplicate runs ($n = 5$). *B*, representative Western blot showing FAHD1, PC, and PEPCK protein levels in liver of *ad libitum* fed, fasted, and refed mice; α-tubulin levels are shown as a loading control. *C*, specific band intensities were quantified using Fiji software and normalized to tubulin. Data are represented as mean ± S.D. ($n = 5$). *, $p < 0.05$; **, $p < 0.01$; ***, $p < 0.001$.

ever currently hypothetical. In a structure-based clustering analysis, FAHD1 clustered together with prokaryotic members of the FAH superfamily, including fumarylpyruvate hydrolases and the oxaloacetate decarboxylase Cg1458 from *C. glutamicum*. Oxaloacetate decarboxylases from prokaryotic organisms are well studied and are either soluble and divalent cation-dependent (like Cg1458) or membrane-bound and dependent on sodium and biotin (20). Molecular modeling based on the established x-ray structure of FAHD1 (9) revealed that indeed the catalytic centers of FAHD1 and Cg1458 are very similar and support a common catalytic mechanism.

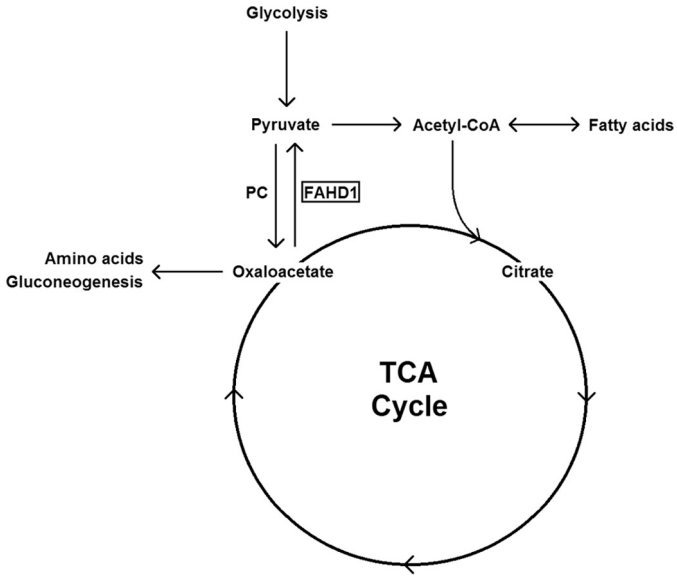

FIGURE 6. **Putative role of FAHD1 in central metabolism as an antagonist of PC.** *TCA cycle*, tricarboxylic acid cycle.

ODx activity in the mammalian organism, especially in regard to mitochondria, has been discussed in a small number of studies, but the majority of these were published many decades ago. The responsible enzyme(s) were detected and characterized in these works, typically from rat liver mitochondria, but not conclusively identified (17, 18, 21). Our own enzymatic studies were performed *in vitro* with recombinantly expressed and purified FAHD1. The catalytic rates we observed may seem low in relation to prokaryotic ODx enzymes like Cg1458 (7), with V_{max} values that are several magnitudes higher, but they compare well with the results from earlier studies on mammalian tissue mentioned above. It seems reasonable that at least some of these earlier studies were actually based on FAHD1, although the enzyme itself was not identified.

Also, it is difficult to judge the actual *in vivo* activity from our *in vitro* results as additional parameters such as cofactors or post-translational modifications could play an important role. To address the question of whether the inclusion of protein tags or recombinant expression in a prokaryotic system might be detrimental to the enzymatic activity of FAHD1, an untagged variant was purified from *E. coli* and a His-tagged variant was obtained from baculoviral expression in SF9 insect cells. These preparations did not differ in their enzymatic properties when tested.[3] The *in vitro* experiments reported here also revealed an inhibitory effect of oxalate on FAHD1 that had already been reported for Cg1458 (8), yielding further evidence for the similarity of their active sites.

PC replenishes oxaloacetate that is withdrawn from the Krebs cycle for biosynthesis in different pathways (19). The tissue-dependent expression pattern of mouse FAHD1 reported here shows correlation with the published expression pattern of PC (22). More importantly, we could observe elevated oxaloacetate levels in FAHD1 knock-out mice, giving reasonable evidence that FAHD1 directly counteracts PC activity, contributing to the balance between pyruvate and oxaloacetate levels (Fig. 6). Although both PEPCK and to a lesser extent PC expression are known to be altered in liver during a fasting cycle

(19, 23), no clear transcriptional regulation could be observed for FAHD1 under these circumstances in mice.

Finally, oxaloacetate is known to act as an inhibitor of several mitochondrial enzymes (18); thus ODx activity might play a vital role in preventing inactivation of metabolic pathways by keeping oxaloacetate levels in check. Additional studies are now required to further elucidate the relevance of FAHD1 for eukaryotic metabolism and to look into possible compensatory mechanisms in the case of FAHD1 depletion.

Acknowledgments—We thank Michael Neuhaus for expert technical assistance. We are grateful to Grit D. Straganz for initial contributions to the FAHD1 project.

REFERENCES

1. Hsiang, H. H., Sim, S. S., Mahuran, D. J., and Schmidt, D. E., Jr. (1972) Purification and properties of a diketo acid hydrolase from beef liver. *Biochemistry* **11,** 2098–2102
2. Phaneuf, D., Labelle, Y., Bérubé, D., Arden, K., Cavenee, W., Gagné, R., and Tanguay, R. M. (1991) Cloning and expression of the cDNA encoding human fumarylacetoacetate hydrolase, the enzyme deficient in hereditary tyrosinemia: assignment of the gene to chromosome 15. *Am. J. Hum. Genet.* **48,** 525–535
3. Mitchell, G. A., Grompe, M., Lambert, M., and Tanguay, R. M. (2001) Hypertyrosinemia. in *The Metabolic and Molecular Bases of Inherited Diseases* (Scriver, C. R., Beaudet, A. L., Sly, W. S., and Valle, D., eds), 8th Ed., pp. 1777–1805, McGraw-Hill, New York
4. Tame, J. R., Namba, K., Dodson, E. J., and Roper, D. I. (2002) The crystal structure of HpcE, a bifunctional decarboxylase/isomerase with a multifunctional fold. *Biochemistry* **41,** 2982–2989
5. Brouns, S. J., Barends, T. R., Worm, P., Akerboom, J., Turnbull, A. P., Salmon, L., and van der Oost, J. (2008) Structural insight into substrate binding and catalysis of a novel 2-keto-3-deoxy-D-arabinonate dehydratase illustrates common mechanistic features of the FAH superfamily. *J. Mol. Biol.* **379,** 357–371
6. Pollard, J. R., and Bugg, T. D. (1998) Purification, characterisation and reaction mechanism of monofunctional 2-hydroxypentadienoic acid hydratase from *Escherichia coli*. *Eur. J. Biochem.* **251,** 98–106
7. Klaffl, S., and Eikmanns, B. J. (2010) Genetic and functional analysis of the soluble oxaloacetate decarboxylase from *Corynebacterium glutamicum*. *J. Bacteriol.* **192,** 2604–2612
8. Ran, T., Gao, Y., Marsh, M., Zhu, W., Wang, M., Mao, X., Xu, L., Xu, D., and Wang, W. (2013) Crystal structures of Cg1458 reveal a catalytic lid domain and a common catalytic mechanism for the FAH family. *Biochem. J.* **449,** 51–60
9. Manjasetty, B. A., Niesen, F. H., Delbrück, H., Götz, F., Sievert, V., Büssow, K., Behlke, J., and Heinemann, U. (2004) X-ray structure of fumarylacetoacetate hydrolase family member *Homo sapiens* FLJ36880. *Biol. Chem.* **385,** 935–942
10. Pircher, H., Straganz, G. D., Ehehalt, D., Morrow, G., Tanguay, R. M., and Jansen-Dürr, P. (2011) Identification of human fumarylacetoacetate hydrolase domain-containing protein 1 (FAHD1) as a novel mitochondrial acylpyruvase. *J. Biol. Chem.* **286,** 36500–36508
11. Zhou, N. Y., Fuenmayor, S. L., and Williams, P. A. (2001) *nag* genes of *Ralstonia* (formerly *Pseudomonas*) sp. strain U2 encoding enzymes for gentisate catabolism. *J. Bacteriol.* **183,** 700–708
12. Berman, H., Henrick, K., and Nakamura, H. (2003) Announcing the worldwide Protein Data Bank. *Nat. Struct. Biol.* **10,** 980
13. Timm, D. E., Mueller, H. A., Bhanumoorthy, P., Harp, J. M., and Bunick, G. J. (1999) Crystal structure and mechanism of a carbon-carbon bond hydrolase. *Structure* **7,** 1023–1033
14. Wolfenden, R., Lewis, C. A., Jr., and Yuan, Y. (2011) Kinetic challenges facing oxalate, malonate, acetoacetate, and oxaloacetate decarboxylases. *J. Am. Chem. Soc.* **133,** 5683–5685
15. Schindelin, J., Arganda-Carreras, I., Frise, E., Kaynig, V., Longair, M., Pietzsch, T., Preibisch, S., Rueden, C., Saalfeld, S., Schmid, B., Tinevez, J. Y., White, D. J., Hartenstein, V., Eliceiri, K., Tomancak, P., and Cardona, A. (2012) Fiji: an open-source platform for biological-image analysis. *Nat. Methods* **9,** 676–682
16. Parvin, R., Caramancion, M. N., and Pande, S. V. (1980) Convenient rapid determination of picomole amounts of oxaloacetate and aspartate. *Anal. Biochem.* **104,** 296–299
17. Corwin, L. M. (1959) Oxaloacetic decarboxylase from rat liver mitochondria. *J. Biol. Chem.* **234,** 1338–1341
18. Wojtczak, A. B., and Walajtys, E. (1974) Mitochondrial oxaloacetate decarboxylase from rat liver. *Biochim. Biophys. Acta* **347,** 168–182
19. Jitrapakdee, S., St Maurice, M., Rayment, I., Cleland, W. W., Wallace, J. C., and Attwood, P. V. (2008) Structure, mechanism and regulation of pyruvate carboxylase. *Biochem. J.* **413,** 369–387
20. Lietzan, A. D., and St Maurice, M. (2014) Functionally diverse biotin-dependent enzymes with oxaloacetate decarboxylase activity. *Arch. Biochem. Biophys.* **544,** 75–86
21. Dean, B., and Bartley, W. (1973) Oxaloacetate decarboxylases of rat liver. *Biochem. J.* **135,** 667–672
22. Ballard, F. J., Hanson, R. W., and Reshef, L. (1970) Immunochemical studies with soluble and mitochondrial pyruvate carboxylase activities from rat tissues. *Biochem. J.* **119,** 735–742
23. Hanson, R. W., and Reshef, L. (1997) Regulation of phosphoenolpyruvate carboxykinase (GTP) gene expression. *Annu. Rev. Biochem.* **66,** 581–611